Transactions of the Korean Nuclear Society Spring Meeting
Jeju, Korea, May 17-18, 2018

A novel scintillator – photodiode detector to detect partial defects of PWR spent fuel assemblies for nuclear safeguards

Haneol Lee[a] and Man-Sung Yim[a*]

[a]*Department of Nuclear and Quantum Engineering, KAIST 291 Daehak-ro, Yuseong-gu, Daejeon, 34141, Republic of Korea*
[*]*Corresponding author: msyim@kaist.ac.kr*

1. Introduction

Nuclear non-proliferation becomes increasingly important as the number of countries with nuclear power increases. Due to technical and practical limitations, nuclear safeguards continues to face challenges as the number of nuclear facilities and the amount of nuclear material to be safeguarded increases. hile Similarly the diversion pathways of nuclear material and inspection time for nuclear material verification also increase. Such challenges are reflected in the creation of research projects, such as the U.S. Department of Energy Next Generation Safeguards Initiative Spent Fuel (NGSI-SF), conducted specifically for establishing the baseline of future nuclear safeguards and non-destructive assay (NDA) detectors.

The objective of nuclear safeguards is "timely detection of diversion of significant quantities of nuclear material and deterrence of such diversion by the risk of early detection", according to the IAEA [1]. To meet the requirements, spent fuel assemblies have to be verified before they are stored in a geological repository or an encapsulation cask [2]. Verification of a spent fuel assembly is accomplished by comparing the amount of declared and existing nuclear material in an assembly [3]. Remaining challenges in nuclear safeguards of spent fuel include improving the capabilities of NDA instruments for partial defect detection, autonomous spent fuel information verification, and plutonium inventory measurement [4]. Partial defect is defined as "an item or a batch that has been falsified to such an extent that some fraction of the declared amount of material is actually present" [3]. Conventional instruments for partial defect detection measure the localized intensity of passive gamma or passive neutrons. Instruments for spent fuel information verification count the passive gamma, passive neutron, or active neutron to measure initial enrichment, burnup, and cooling time. Instruments for plutonium inventory verification count active neutrons since Cm244 dominates passive neutrons from spent fuel. Since there is no quantified or declared objective for detection limits in the literature, partial defect detection remains particularly challenging in NDA instrument development.

There are a number of NDA instruments designed to detect partial defects. These instruments, include the digital Cerenkov viewing device (DCVD), fork detector (FDET), partial defect detector (PDET), passive gamma emission tomography (PGET), or spent fuel MOX python (SMOPY) [2, 3, 5]. These instruments distinguish defective spent fuel assemblies from normal spent fuel assemblies by using a combination of neutron and gamma detection, multiple gamma detectors, or by visualization of photon intensity. These methods are summarized in Table 1.

Unfortunately, these methods still present limitations which include poor spatial resolution for detecting partial defects, long detection time, poor cost effectiveness, or high maintenance requirements. In particular, these NDA instruments require calibrating count rate, especially for passive gamma. The calibration process delays inspection time and requires the presence of an inspector or operator, which prohibits autonomous spent fuel verification. The characteristics and limitations of conventional instruments are described in Table 1.

Table 1. Characteristics of conventional NDA instruments for partial defect detection.

Detector	Methods	Limitations
DCVD [6]	Detects local Cerenkov radiation intensity out of cooling pool	1) Spent fuel out of cooling pool cannot be verified 2) Hard to distinguish activated material
FDET [7]	Detect passive gamma and neutron around an assembly	1) Requires spent fuel movement 2) Poor spatial resolution for partial defect detection
PDET [8]	Detect passive gamma and neutron inside guide tubes	1) Poor costs effectiveness 2) Poor cost effectiveness 3) Requires frequent calibration
PGET [9]	1) Detect passive gamma around an assembly 2) Reconstruct a tomographic image	1) Requires spent fuel movement 2) Poor cost effectiveness 3) Long detection time
SMOPY [10]	Measure passive neutron right next to an assembly	1) Requires spent fuel movement 2) Poor cost effectiveness

2. Methods and Results

2.1. Methods of SPDD based partial defect detection

Conventional detectors for spent fuel verification were initially designed to verify spent fuel burnup information. The verification capability of detectors were mainly focused on gross defect detection or burnup estimation. Some detectors which satisfy all kinds of verification capability have limitations, such as long detection time and too expensive detector cost. This research tried to solve this limitation by dividing the verification process into two steps. First process is to verify the consistency of a declared assembly and existing assembly. Once suspicious assemblies are selected by the first process, detailed conventional verification processes are applied to the suspicious assemblies. The only goal of a novel detector in this research is fast and simple verification of spent fuel rod diversion. Since the existence of fuel rods can be verified by local passive gamma detection, a novel detector measures passive gamma at guide tube locations of a fuel assembly. The detector in this research measures local passive gamma intensity inside guide tubes of a spent fuel assembly by a radiation conversion into electric current. Since intensity spent fuel passive gamma intensity is high enough, it is possible to convert passive gamma into detectable electric current.

A scintillator – photodiode based method converts passive gamma into electric current using the following method. The scintillator first converts passive gamma into visible photons. The generated photons are then converted into electric current via a photodiode. Each scintillator – photodiode detector is located inside each guide tube. Since passive gamma from spent fuel rods is attenuated by neighboring fuel rods and assembly structural materials, the generated current at each guide tube location represents local passive gamma intensity and can be used to detect dummy fuel rods.

Figure 1 and 2 provide flowcharts depicting the initial and regular verification process, for using an SPDD. Initially, the SPDD current distribution at each guide tube location is estimated using the operator declared information. Then the real current distribution is measured using the SPDD. Then inspectors inter-compare the estimated and measured current distribution.

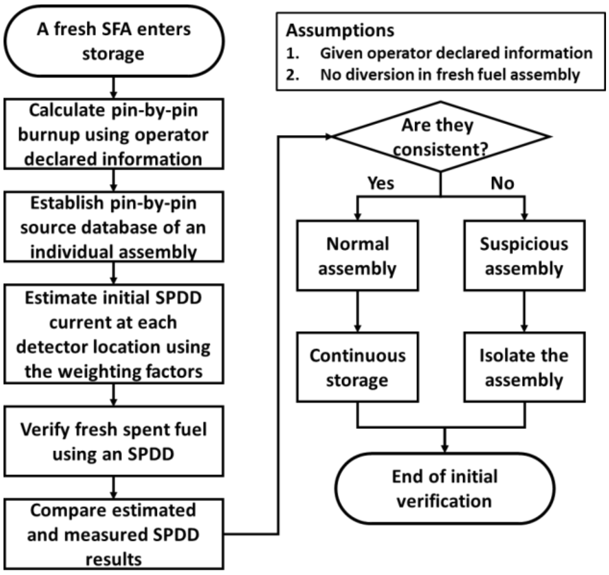

Fig. 1. Flowchart of SPDD based initial spent fuel verification process.

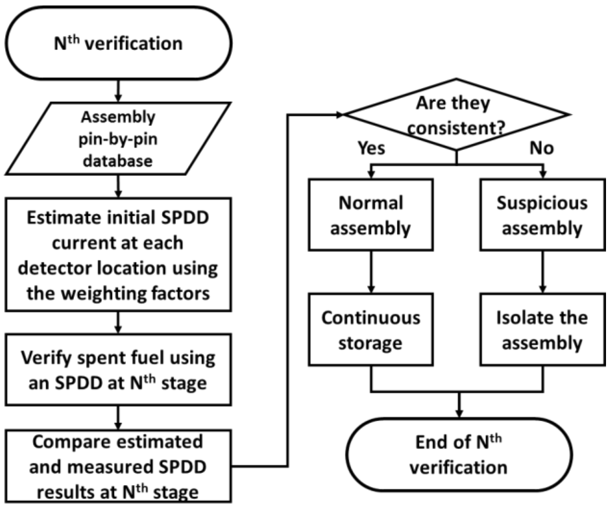

Fig. 2. Flowchart of SPDD based regular inspection process.

2.2. Design of SPDD

The SPDD must perform adequately in the assemblies which store the long-cooled fuel because these assemblies are most vulnerable to partial defects. This research selected a Westinghouse 14x14 type fuel assembly as a target assembly since the assembly is a typical old PWR spent fuel assembly in Republic of Korea.

Figures 3 is a graphic depiction of an SPDD detector design. Figures 3 the scintillator – photodiode detector is referred to as a detector leg. A detector leg includes a single scintillator – photodiode detector, cable, and surrounding structural material. The photodiode cover is cylinder shaped and surrounds the scintillator. A cable connects the top of a scintillator – photodiode detector to a currentmeter. The top and bottom surface of scintillator cylinder are covered by aluminum reflectors to guide the scintillated photons to the photodiode. The whole side of the detector structure is covered by a stainless steel shielding structure. The bottom of a detector leg includes an additional 5cm stainless steel shielding to buffer the potential impact that may occur between the guide tube and the detector leg, during insertion. Each detector leg is positioned at the center of an active fuel length. The radius of the detector leg was designed to have a 2mm gap between interior of the guide tube and the detector leg. The height of the scintillator cylinder and photodiode is 10cm. The thickness of both the photodiode and shielding structure are 1mm. The aluminum reflector is 0.1mm.

This research selected $CdWO_4$ scintillator and amorphous silicon type photodiode due to their high radiation resistance and energy adequacy. Feasibility of applying $CdWO_4$ scintillator in spent fuel storage environment was demonstrated by lab scale experiments by comparing the generated current before and after a number of gamma and neutron irradiations [11].

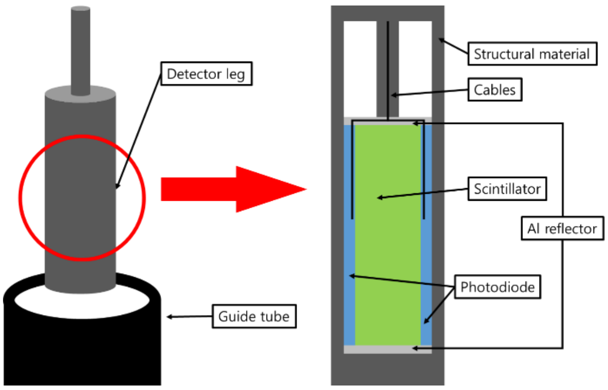

Fig. 3. Design of single SPDD detector leg.

2.3. Test case based SPDD performance analysis

This research setup two real spent fuel assemblies with partial defects (Westinghouse 14x14 type) from literature [12]. The pin-by-pin burnup information of two test case assemblies are calculated by the SCALE code package using operator declared information. The geometry and pin-by-pin burnup distribution of two test case assemblies are depicted in the Figure 4. Red colored fuel pins are the location of dummy fuel rods. This research analyzed the amount of generated current of the two assemblies using a computational model developed in previous study [11].

The effect of single fuel rod diversion on SPDD generated current has to be demonstrated to estimate SPDD current distribution at each guide tube location using pin-by-pin burnup distribution, defined as a weighting factor of pin diversion. This research defined fuel rods located within the third ring from a guide tube as effective fuel rods. The effective fuel rods were classified into "a" to "i" depending on guide tube – fuel rod distance (Figure 5). The weighting factors are calculated by comparing a reference assembly and assemblies with various single fuel rod diversion cases. This research averaged 17 test case assemblies to and averaged all test cases. Results of estimated weighting factors are described in Table 2.

29.9	29.9	29.9	32.0	32.0	32.0	32.8	32.8	33.6	33.6	33.6	34.2	34.2	34.2
29.9	31.7	31.7	31.7	33.2	33.2	34.0	34.0	34.9	34.9	35.1	35.1	35.1	34.2
29.9	31.7		33.6	33.6		34.0	34.0		35.8	35.8		35.1	34.2
29.9	31.7	33.6	33.6	33.6	33.6	34.0	34.0	35.8	35.8	35.8	35.8	35.1	33.9
29.9	31.8	33.6	33.6		33.6	33.1	33.1	35.8		35.8	35.8	35.1	33.9
29.9	31.8		33.6	33.6	33.6	33.1	33.1	35.8	35.8	35.8		35.1	33.9
28.3	31.2	31.2	31.2	31.8	31.8		33.3	33.2	33.2	34.2	34.2	34.2	33.1
28.3	31.2	31.2	31.2	31.8	31.8	33.3	33.3	33.2	33.2	34.2	34.2	34.2	33.1
27.5	30.2		31.5	31.5	31.5	31.8	31.8	33.7	33.7	33.7		33.5	32.4
27.5	30.2	31.5	31.5		31.5	31.8	31.8	33.7		33.7	33.7	33.5	32.4
27.5	28.3	31.5	31.5	31.5	31.5	31.1	31.1	33.7	33.7	33.7	33.7	31.8	32.4
26.0	28.3		31.5	31.5		31.1	31.1		33.7	33.7		31.8	30.0
26.0	28.3	28.3	28.3	30.0	30.0	31.1	31.1	31.7	31.7	31.8	31.8	31.8	30.0
26.0	26.0	26.0	27.2	27.2	27.2	27.9	27.9	28.6	28.6	28.6	30.0	30.0	30.0

C15

28.2	27.8	27.5	27.3	27.1	27	26.9	25.4	25.3	25	24.6	24	23.2	22.3
29.6	29.5	29.7	29.1	28.8	29.2	28.7	27.1	27.4	26.8	28.3	26	24.8	23.6
31	31.4		31.3	31.1		30.7	29		28.8	28.3		26.5	24.8
32.1	32.2	32.8	32.5	32.8	32.5	31.5	29.6	30.3	30.2	29.3	28.7	27.2	25.8
33.2	33.4	34	34.2		33.4	32.4	30.1	30.9		30.7	29.7	28.1	26.7
34.3	34.9		35	34.5	34	34	30.9	30.9	31.3	31.2		28.2	27.4
35.1	35.2	35.7	34.9	34.4	34.9		31.8	31	30.9	30.9	30.7	29.3	27.9
36.2	36.3	36.8	35.9	35.2	34.9	35	34.4	33.8	33.6	33.5	33.3	31.7	30.3
37	37.7		37.8	37	35.8	35	34.7	34.8	35.2	35.1		32.8	30.9
37.7	38	38.7	38.8		37.3	35.9	35.5	38.3		36	34.8	32.9	31.4
38.5	38.7	39.4	39	39.2	38.3	37.2	36.8	37.6	37.3	36.2	35.4	33.6	32.1
39.2	39.9		39.8	39.5		38.6	38.2		37.7	37		34.8	32.9
39.7	39.8	40.2	39.4	39.1	39.3	38.4	38.2	38.5	37.5	36.9	36.6	35	33.6
40.3	40	39.7	39.4	39.1	38.8	38.5	38.6	38.3	37.8	37.2	36.5	35.5	34.6

G23

Fig. 4. Geometry of test case spent fuel assemblies with partial defects (Top: C15 (KORI1), Bottom: G23 (KORI1))

I	H	G	F	G	H	I
H	E	D	C	D	E	H
G	D	B	A	B	D	G
F	C	A	GT	A	C	F
D	G	B	A	B	D	G
H	E	D	C	D	E	H
I	H	G	F	G	H	I

Fig. 5. Effective fuel rod for a single SPDD detector (GT: guide tube, A~I: Effective fuel rod location)

Table 2. Calculated weighting factors for nine fuel rod – guide tube distances

w_A	w_B	w_C	w_D	w_E	w_F	w_G	w_H	w_I
29.43	20.30	4.740	10.44	3.180	1.630	5.228	1.713	1.000

The performance of an SPDD was analyzed by comparing the estimated current distribution (without partial defects), model calculated distribution (without partial defects), and model calculated distribution (with partial defects). The six cooling time cases (5, 10, 15, 20, 30, 50 year) were selected to describe continuous inspections. The estimated current distribution was only compared to the model calculated distribution (without partial defect) at initial storage since diverting nuclear material from fresh spent fuel assembly is hardly to occur. Once the consistency between the estimated and model calculated current distribution is verified, this research compared the model calculated current distribution between without partial defects and with partial defects for the six different cooling times.

The estimated current distribution and modeled current distribution of the two assemblies (C15 and G23) without defects are depicted in Figure 6 and 7. The estimated and modeled distribution are consistent as illustrated in Figure 6. This result indicate the calculated weighting factors are precise values. The differences between the estimated and modeled distribution occurred in the SPDD detectors located at corner guide tubes. Reason of the differences is the corner guide tubes do not have entire effective fuel rods. Future works need to adjust this difference.

The difference between the estimated and modeled current distribution for the two assemblies are depicted in Figure 8 and 9. Since the location of dummy fuel rods are consistent within the same assembly, SPDD current distributions for different cooling times are consistent within the same assembly. Figure 7 and 8 depicts the results of 20 year cooling time. As illustrated in the figure, SPDD can distinguish both test case assemblies with partial defects.

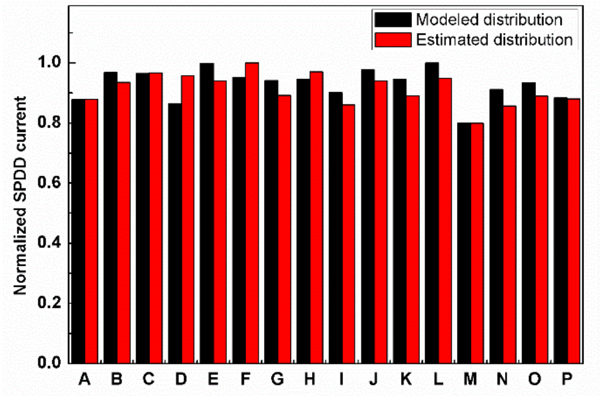

Fig. 6. Estimated and modeled initial current distribution of C15 assembly.

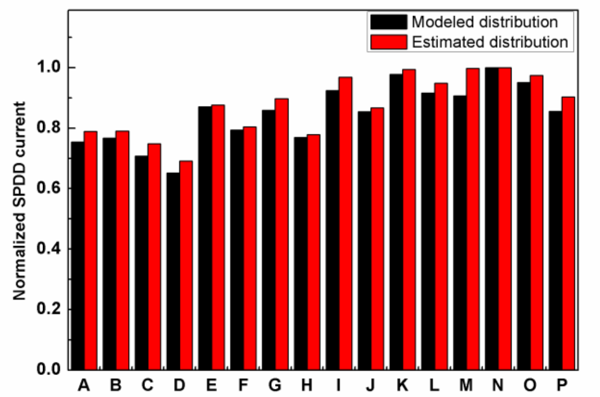

Fig. 7. Estimated and modeled initial current distribution of G23 assembly.

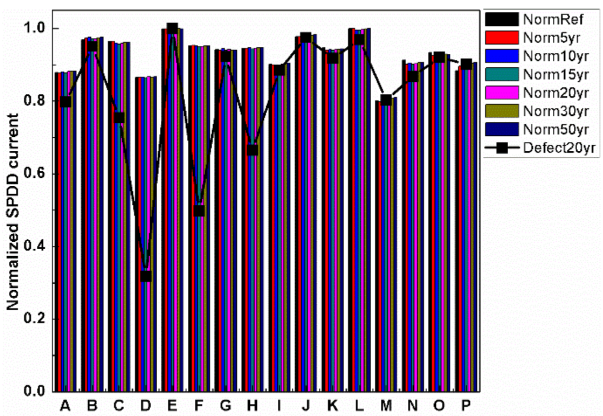

Fig. 8. Modeled current distribution of normal C15 spent fuel assembly (5~50 year cooling) and assembly with partial defects after cooled for 20 years.

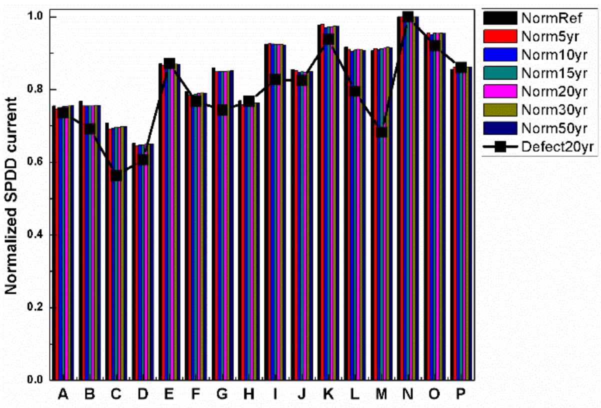

Fig. 9. Modeled current distribution of normal G23 spent fuel assembly (5~50 year cooling) and assembly with partial defects after cooled for 20 years.

3. Conclusions

This research suggested a novel scintillator – photodiode based detector for verifying partial defects of PWR spent fuel assemblies. Investigation of detection method and system design were included in this research. Furthermore, system feasibility was demonstrated using test case assemblies with real partial defects. Results indicate the system can distinguish defective assemblies from normal assemblies.

Future studies will include a quantitative uncertainty analysis as well as system evaluation. Detection criterion setup and detection resolution evaluation will be conducted after the quantitative uncertainty analysis. Overall evaluation of system performance will be conducted after comparing SPDD and conventional detectors for partial defect verification.

REFERENCES

[1] International Atomic Energy Agency (IAEA), The structure and content of agreements between the agency and states required in connection with the treaty on the non-proliferation of nuclear weapons, INFCIRC/153 (corrected), 1972

[2] M. Tarvainen, F. Levai, T. E. Valentine, M. Abhold, and B. Moran, NDA techniques for spent fuel verification and radiation monitoring, STUK-YTO-TR-133, 1997

[3] International Atomic Energy Agency (IAEA), Safeguards techniques and equipment: 2011 edition, IAEA-NVS-3, 2011.

[4] J. Hu, I. C. Gauld, J. E. Banfield, and S. E. Skutnik, Developing Spent Fuel Assembly Standards for Advanced NDA Instrument Calibration –NGSI Spent Fuel Project, ORNL/TM-2013/576, 2014.

[5] B. Siskind, Measurement of spent fuel assemblies overview of the status of the technology for initiating discussions at National Research Centre Kurchatov Institute, BNL-101126-2013-IR, 2013.

[6] J. D. Chen, D. A. Parcey, and R. Kosiery, Detection of partial defects using a digital Cerenkov viewing device, IAEA-CN-184/338, 2010.

[7] S. J. Tobin and P. Jansson, Nondestructive assay options for spent fuel encapsulation, SKB-TR-13-30, 2013.

[8] Y. Ham, P. Kerr, S. Sitaraman, R. Swan, R. Rossa, and H. Liljenfeldt, Partial defect verification of spent fuel assemblies by PDET: Principle and Field testing in Interim spent fuel storage facility (CLAB) in Sweden, ANIMMA, 2015 4th International Conference on. IEEE, 2015.

[9] S. Holcoombe, S. J. Svard, and L. Hallstadius, A novel gamma emission tomography instrument for enhanced fuel characterization capabilities within the OECD HaldenReactor Project, Annals of Nuclear Energy, 85, 834-845, 2015.

[10] A. Lebrun, M. Merelli, J. L. Szabo, M. Huver, R. Arlt, and J, Areans-Carrasco, SMOPY a new NDA tool for safeguards of LEU and MOX spent fuel.,International Atomic Energy Agency Report IAEA-SM-367/14/03 47, 2003.

[11] H. Lee and M. S. Yim, Examination of scintillator-photovoltaic cell-based spent fuel radiation energy conversion for electricity generation, Progress in Nuclear Energy, (94), 46-54, 2017.

[12] Ref_Ham 2009